Ovarian Cancer Detection Using Hyperpolarized ^{13}C-Pyruvate with MR Imaging and Spectroscopy

Mehrdad Pourfathi[1,2], Stephen J. Kadlecek[1], Harrilla Profka[1], Hoora Shaghaghi[1], Moses Darpolor[1], Kiarash Emami[1], Nicholas N. Kuzma[1], Jan H. Ardenkjær-Larsen[3], Rahim R. Rizi[1], and Janet A. Sawicki[4]

[1]Radiology, University of Pennsylvania, Philadelphia, PA, United States, [2]Electrical and Systems Engineering, University of Pennsylvania, Philadelphia, PA, United States, [3]GE Healthcare, Brøndby, Denmark, [4]Lankenau Institute for Medical Research, Wynnewood, PA, United States

Introduction: Ovarian cancer is the fifth most common cancer in the US women with approximately 25,000 newly diagnosed cases of ovarian carcinoma, coupled with high fatality of 14,000 deaths each year. The survival rate, if diagnosed at early stages is approximately 90%. But, due to the asymptomatic nature of the disease at early stages and the lack of effective screening modalities, most women are not diagnosed until the cancer has reached an advanced stage and has metastasized beyond the ovary. Lactate dehydrogenase (LDH), the enzyme that catalyzes the inter-conversion of lactate and pyruvate in the glycolysis pathway, has been shown to be unregulated in ovarian cancer, which may result in elevated lactate concentrations in the tumors [1]. The use of hyperpolarized ^{13}C to highlight lymphoma and prostate tumors using MRSI [2] suggests a similar utility to detect small, early-stage ovarian tumors. In the analysis performed for this study, we sought to distinguish between (a) elevated levels of LDH activity, causing a more rapid approach to the equilibrium lactate:pyruvate ratio, and (b) a skewing of the ratio itself, due to shifts in the redox state or other factors selectively favoring the forward pyruvate → lactate reaction over the reverse reaction. Chemical shift imaging, performed several to several tens of seconds after the injection, is commonly used to localize regions of elevated lactate, but cannot distinguish these two situations.

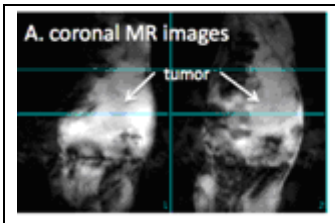

Figure 1: Proton images showing the coronal (A) and axial (B) cross-sections of two tumor-bearing mice at the slice (area between two horizontal green lines in A, images in B) selected for spectroscopy. Note that although some normal tissue appears in the slice as well, tumors are large enough (~1 cm) that the preponderance of signal is expected to arise there due to their size and elevated perfusion/metabolism.

Materials and methods: All animal experiments were performed under an IACUC-approved protocol at the University of Pennsylvania. Three transgenic mice (MISIIR/Tag) developed spontaneous bilateral epithelial ovarian tumors at approximately 18 weeks and were imaged at approximately 30 weeks; three age-matched B6 non-transgenic mice were imaged as controls. All mice were sedated and maintained with isoflurane while a tail-vein catheter was inserted for agent injection. After insertion into the magnet, respiration was monitored and temperature was controlled with forced air heating. 28.5 µg of [1-^{13}C] pyruvic acid was polarized to ~25% using a HyperSense DNP polarizer, then dissolved in 3.4 ml of buffered solution containing stoichiometric NaOH and 100 mg/L EDTA. 10 µl/g-body-weight of hyperpolarized Na pyruvate solution was injected into the tail-vein catheter over ten seconds, followed by a series of slice-selective spectral acquisitions. Spectroscopy was performed with an M2M 35 mm birdcage dual-tuned ^{13}C/^{1}H coil using a 4.7 Tesla Varian imaging magnet with a nominal 20° flip angle applied every second. In each case, a single 8-mm slice was positioned to cover the (bilateral) tumors or the corresponding region of the healthy mice (Fig. 1). A custom Matlab program was used to apply proper zero- and first-order phase correction, baseline removal and spectral line broadening to the acquired data and built-in fitting functions were used to fit Lorentzian lineshapes to the peaks corresponding to pyruvate and lactate. We used a simple model which incorporates the forward and backward conversion of pyruvate/lactate in its steady state due to metabolism as well as spin lattice relaxation of the pyruvate polarization over time using the equations (1) and (2) below, wherein [*lac*] is the lactate signal amplitude, [*pyr*] is the pyruvate signal amplitude, k_+ is the forward (pyruvate→lactate) reaction rate, k_- is the backward reaction rate, and $\Gamma=1/T_1$ represents the relaxation rate.

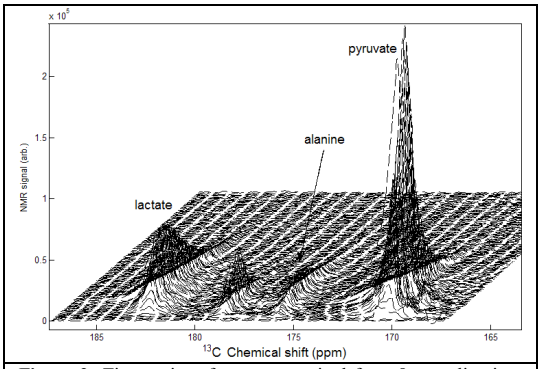

Figure 2: Time-series of spectra acquired from 8-mm slice in a representative tumor-bearing animal

$$\frac{d[lac]}{dt} = k_+[pyr] - k_-[lac] - \Gamma \quad (1) \qquad \frac{d[pyr]}{dt} = -k_+[pyr] + k_-[lac] - \Gamma \quad (2)$$

In performing the fit, [*pyr*] was set to the measured pyruvate peak amplitude for the first twenty seconds (during which agent inflow and uptake was significant and not reproducible); whereas all [*lac*] and the subsequent [*pyr*] evolution was according to Eq. 1-2.

Results and discussion: Fig. 2 shows a representative time-series of spectra acquired from a tumor-bearing animal. Four peaks (pyruvate, pyr-hydrate, alanine, and lactate) are always distinguishable. Figures 3.A1-A3 show the time-series of peak amplitudes in control animals. With the exception of the third animal, we observed markedly lower lactate levels when compared to the three bottom figures (B1-B3), which correspond to tumor cases. We find that the model always fits the observed evolution very well, and the extracted forward and backward pyruvate/lactate conversion rates (Table 1) show larger values for tumor-bearing animals (notably so when forward and backward rates are summed). This suggests that overall LDH activity in the tumor is elevated, perhaps in addition to favoring the forward reaction, although our small sample size does not yet allow statistically significant conclusions. We do not yet know the reason for high apparent lactate production in the third control, but believe that significant in-slice contamination from the kidneys is likely; the organs are very close and it is often impossible to choose a slice passing through the ovaries without admitting a significant contribution from the more metabolically active kidney.

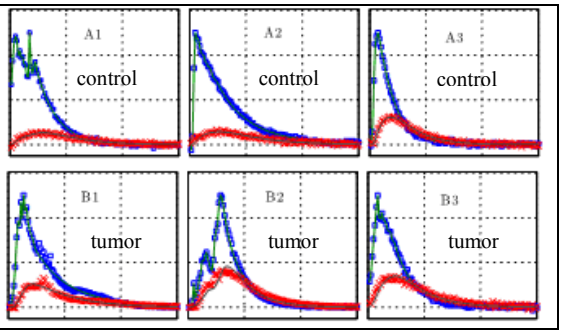

Figure 3: Spectral peak amplitudes corresponding to pyruvate (blue) and lactate (red) and the associated model fits (green curves). All time axes cover 120 seconds (dashed lines are at 40 s and 80 s) and spectral series are normalized to have the same maximum pyruvate peak height.

Conclusion and future directions: We observed higher level of LDH activity (in both directions) associated with ovarian-tumor-bearing animals. The model used to extract the apparent rate constants allows for extraction of both forward and reverse rate constants, but requires high signal-to-noise ratio, particularly at late times; this is likely not practical with CSI or other localization. The model does not explicitly take into account uptake or transport, and does not allow for differing relaxation characteristics. These additions, along with a greater sample size, are the subject of future investigations.

Experiment	Controls			Tumors		
	A_1	A_2	A_3	B_1	B_2	B_3
k_+ (s^{-1})	0.0119	0.0174	0.0446	0.0410	0.0758	0.0442
k_- (s^{-1})	-0.0020	0.0406	0.0221	0.0808	0.0823	0.0337
k_{tot}	0.0099	0.0580	0.0666	0.1218	0.1581	0.0778

Table 1: Estimated forward and backward pyruvate/lactate conversion rates.

References: [1] D. Schneider et al., Gynecol. Oncol. 66:399-404 (1997). [2] K. Golman, et al., Br. J. Radiol. 76:S118-S127 (2003).